Shear-Induced Conformational Ordering, Relaxation, and Crystallization of Isotactic Polypropylene

Haining An,[†,‡] Xiangyang Li,[†] Yong Geng,[§] Yunlong Wang,[†] Xiao Wang,[†] Liangbin Li,[*,†] Zhongming Li,[‡] and Chuanlu Yang[§]

National Synchrotron Radiation Laboratory and Department of Polymer Science and Engineering, University of Science and Technology of China, Hefei, China, College of Polymer Science and Engineering and State Key Laboratory of Polymer Materials Engineering, Sichuan University, Chengdu, China, and Department of Physics and Electrons, Ludong University, Yantai, China

Received: March 22, 2008; Revised Manuscript Received: July 30, 2008

The shear-induced coil−helix transition of isotactic polypropylene (iPP) has been studied with time-resolved Fourier transform infrared spectroscopy at various temperatures. The effects of temperature, shear rate, and strain on the coil−helix transition were studied systematically. The induced conformational order increases with the shear rate and strain. A threshold of shear strain is required to induce conformational ordering. High temperature reduces the effect of shear on the conformational order, though a simple correlation was not found. Following the shear-induced conformational ordering, relaxation of helices occurs, which follows the first-order exponential decay at temperatures well above the normal melting point of iPP. The relaxation time versus temperature is fitted with an Arrhenius law, which generates an activation energy of 135 kJ/mol for the helix−coil transition of iPP. At temperatures around the normal melting point, two exponential decays are needed to fit well on the relaxation kinetic of helices. This suggests that two different states of helices are induced by shear: (i) isolated single helices far away from each other without interactions, which have a fast relaxation kinetic; (ii) aggregations of helices or helical bundles with strong interactions among each other, which have a much slower relaxation process. The helical bundles are assumed to be the precursors of nuclei for crystallization. The different helix concentrations and distributions are the origin of the three different processes of crystallization after shear. The correlation between the shear-induced conformational order and crystallization is discussed.

Introduction

Flow fields are inevitably applied during polymer processing. The development of order under such conditions has attracted considerable interests.[1−3] Polymer order comprises intermolecular positional and orientational orders as well as intramolecular conformational order.[4,5] These two types of order can be properly studied independently during shear-induced crystallization of polymers, provided the intermolecular and intramolecular order can be decoupled.[6,7] In a former paper,[8] we showed that the shear field leads to an increase of both the concentration and the length of helices in isotactic polypropylenes (iPP) melt and found that the destinies of the conformational order after shear strongly depend on temperature. The shear-induced conformational ordering, relaxation, and crystallization is further reported in this work. We intend to reveal how shear field influences conformational ordering and how these conformational ordered segments organize and affect crystallization.

Theory about the stretch-induced coil−helix transition of a single chain has been formulated by Buhot and Halperin[9,10] and Tamashiro and Pincus,[11] in which the end-to-end distance r of a chain is the essential parameter to shift the ratio between helix and coil. This theory was further extended to a multichain network by Courty et al.,[12,13] which was also tested by their experiments on gelatin. The basic idea of this theory can be borrowed for the shear-induced coil−helix transition in polymer melts, provided the relaxation is taken into account. As a polymer melt is a transient network constructed with entanglements, competition between the shear-induced orientation or stretch and relaxation with a time scale of reptation τ_r or Rouse time τ_R always exists. Thus, extension of the end-to-end distance R induced by shear is not only determined by shear strain but also by shear rate and temperature.

After the cessation of shear, the induced helices will experience a reorganization or relaxation, which is determined by temperature and the state of the helices. This question is directly related to the structure of the so-called precursor of crystallization. Observation of flow-induced long-living metastable structures in crystallizable polymer melts at high temperatures has recently been reported by several groups.[14−26] Rheo−Raman experiments showed that flow promotes the formation of all-trans sequences which have a lifetime up to several hours after the cessation of flow.[16] Density fluctuations have been proved to appear earlier than crystalline structures[17−19] Shear-induced orientational ordering represented with an upturn in birefringence has been reported by Kornfield's group[20,21] in iPP melt at a high temperature of 175 °C after shear. Somani and co-workers[22−26] argued that metastable noncrystalline aggregates were generated through assembling of oriented chain segments in sheared iPP, which was characterized as a layerlike superstructure. Though the shear-induced structures survive for a considerable duration of time in the melt, systematic studies of their relaxation behavior and thermal stability are still rare. In this regard, the studies of Azzurri and Alfonso[27] and Zuo et

* Corresponding author. E-mail: lbli@ustc.edu.cn.
† University of Science and Technology of China.
‡ Sichuan University.
§ Ludong University.

10.1021/jp802511b CCC: $40.75
Published on Web 09/06/2008

al.[28] deserve a special mention. In a series of well-designed experiments, they systematically investigated the relaxation behavior of shear-induced precursors in isotactic poly(1-butene) (iPB) and polyethylene (PE) melts, respectively.

What is the initial structure of the shear-induced precursor?[25] Due to lacking precise order parameters, the concept of the precursor is vague and has been questioned in the community for a long time. To depict the nuclei or precursor at the molecular level is difficult because they take a very small volume fraction at the early stages of crystallization and give a weak signal. Interchain ordering such as orientation and density fluctuation has been emphasized in many reported works, which implies that the precursors contain multistems instead of an isolated single segment. On the other hand, conformational order seems to be a necessary condition for the occurrence of the precursors. Segments with ordered conformation such as helix possess the so-called induced rigidity,[29,30] which can promote the orientational order and interchain close packing. Investigations of the chain conformation suggest that the transformation to a denser, oriented transient phase is associated with conformational changes.[31−33] Combining time-resolved small-angle X-ray scattering (SAXS) and Fourier transform infrared (FTIR) data of PE during the isothermal crystallization from the melt, Tashiro and co-workers[33,34] argued that conformational ordering and lamellar formation follow three time regions.

The aim of the present study is to extend the above investigations and try to probe the nature of the precursors in the viewpoint of conformational order. How the precursor relates to the shear-induced coil−helix transition is the essential question we would like to answer. FTIR spectroscopy was employed to follow the shear-induced coil−helix transition of iPP, because knowledge about the conformational characteristics of iPP[35,36] and the relationship between the helical length of iPP segments and certain absorption bands in infrared spectra have been well documented.[37−41] The IR bands at 940, 1220, 1167, 1303, 1330, 841, 998, 900, 808, 1100, and 973 cm^{-1} correspond to helical structures with degree of order from high to low, and the minimum n values for appearance of bands at 973, 998, 841, and 1220 cm^{-1} are 5, 10, 12, and 14 monomers in helical sequences, respectively.[40,41] Shear-induced conformational ordering and relaxation were studied. The relaxation and subsequent crystallization suggest that the precursors are helical bundles with conformational ordered multistems.

Experimental Section

High-molecular-mass iPP, supplied by SABIC−Europe, had a melt flow index of about 0.3 g/10 min (230 °C/2.16 kg, ASTM D1238) and an average M_n and M_w of about 150 and 720 kg/mol, respectively. The melting point was around 165 °C. For the shear experiments iPP discs were prepared from the pellets as received as well as powder extracted and washed from xylene solution with acetone. No difference was found between these two starting materials.

To impose a shear field, a homemade parallel plate cell driven by a servomotor was employed. Two ZnSe plates were used as IR windows enclosing an iPP sample of 350 μm thickness. The samples were first heated up to 220 °C for 5 min to erase possible memory effects, then cooled down to the required temperature T_s, and held for 15 min before shear. In situ IR spectra were collected over a wavenumber range of 400−4000 cm^{-1} using a Bruker TENSOR 37 FTIR spectrometer with a resolution of 4 cm^{-1}.

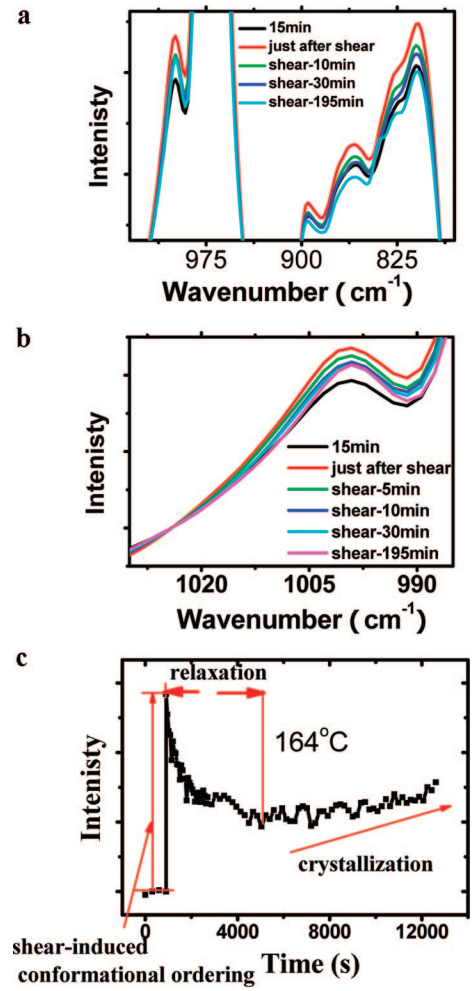

Figure 1. (a) IR spectra of iPP at 164 °C before and after shear; (b) IR spectra of the 998 cm^{-1} band at 164 °C before and after shear. (c) Intensities of the 998 cm^{-1} band vs time at 164 °C.

Results

Shear-Induced Conformational Ordering. Figure 1a gives representative IR spectra before and after shear at 164 °C at the time indicated. The intensities given refer to the peak height above the baseline after careful baseline subtraction rather than peak area. Here the 1024 cm^{-1} band was chosen because it is the lowest point between the two fully grown peaks (1055 and 998 cm^{-1}), making it suitable even at low temperatures when there is a small peak at 1055 cm^{-1}. Different authors may find a different "the lowest point" for the absorption band and apply as baseline correction. This may shift the absolute value of the peak height but does not influence the general trend. By simply applying only one baseline standard rather than choosing different standards in different situations, we can have the possible artifacts from baseline correction removed.

The intensity change is conformation itself rather that the variation of thickness. As mentioned in our previous paper,[8] all conformational bands show an increased intensity after shear except the 973 cm^{-1} band, as it is recognized as the amorphous band. It is also safe to use the relative intensity between the helical band and amorphous band, and similar results are gotten. The intensity change due to conformational ordering was further supported by the intensity evolution of different conformational bands as they follow a different relaxation process after shear. Helices with about six monomers, represented by the 1100 cm^{-1} band, have a larger response to shear and a slower relaxation

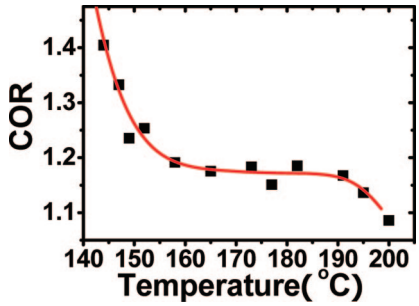

Figure 2. Conformational order ratio (COR) of the 998 cm^{-1} band vs temperature just after shear (shear rate of 13.5 s^{-1}, and shear strain of 3375%).

rate than the longer helix (10 monomers) conformational band at 998 cm^{-1} (Figure 3 of ref 8).

We focus on the 998 cm^{-1} band, which indicates helices with monomer number $n \approx 10$. It was chosen for the convenience of quantitative analysis compared to other conformational bands which correspond to a long helix. As seen from Figure 1b, shear leads to a sharp increase in intensity of the band, revealing a strong enhancement of the corresponding long helices by imposing the flow field. The increase of intensity is attributed to the increase of helical population rather than orientation, since the conformational bands with polarization directions parallel and perpendicular to the helix axis all show an increase of intensity after shear.[42]

Figure 1c gives the variation of the relative intensities of the 998 cm^{-1} band with time at 164 °C. The intensity of the vibration band after shear first goes through a fast decrease, followed by a slow one, and then shows an inflection point which can be understood on the basis of the competition of "melting" of the helical structures and crystallization of the polymer. This phenomenon can be extended to a wide temperature range below the melting point. Other temperatures are not listed for conciseness. There are mainly four parameters which depict a typical relaxation curve of shear-induced conformational order before crystallization: (i) the total amount of shear-induced conformational ordering; (ii) the relaxation time (also the induction time before the crystallization); (iii) relaxation kinetics; (iv) how much induced conformational order still exists after relaxation.

The temperature effect on the shear-induced conformational order is illustrated in Figure 2. The conformational order ratio (COR), defined as the band height ratio of the 998 cm^{-1} band after and before shear, was employed to quantify the effect of shear on conformational order. With the same shear field (shear rate of 13.5 s^{-1} and shear strain of 3375%), the enhancement of the intensity is clearly observed at low temperatures, which becomes smaller at higher temperatures. There is hardly any detectable change above 205 °C (also evidenced in Figure 5 of ref 8).

The effect of shear on conformational order is further studied with different shear strains and rates, respectively. Figure 3 presents the effect of shear strain on the conformational order. A relatively high temperature (145 °C) is chosen to avoid the kicking-in of fast crystallization just after shear which leads to the conformational band continuously increasing and may give some false result. A constant shear rate of 6 s^{-1} is used. With an increase of the strain, the shear-induced COR increases. A minimum shear strain seems to be required to significantly affect the conformation of chains, whereas further increasing the shear strain reaches a saturation of the COR.

The effect of shear rate on the conformational order at three different temperatures is shown in Figure 4. At high temperature,

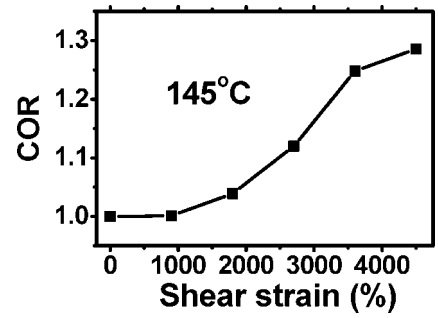

Figure 3. Conformational order ratio (COR) of the 998 cm^{-1} band vs shear duration just after shear (shear rate 6 s^{-1}, and $T = 145$ °C).

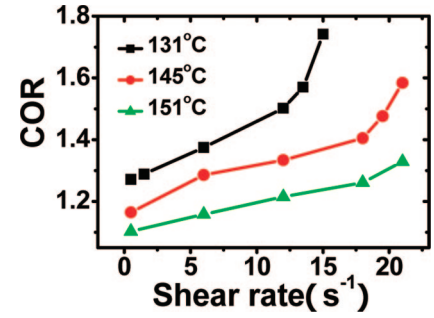

Figure 4. Conformational order ratio (COR) of the 998 cm^{-1} band vs shear rate just after shear at the different temperatures indicated (shear strain of 4500%).

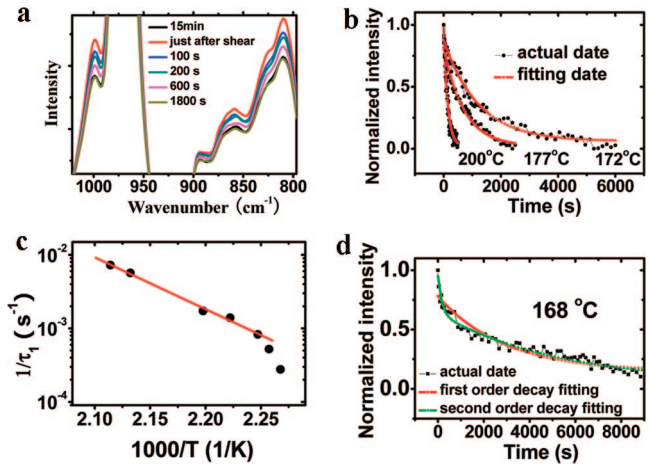

Figure 5. (a) IR spectra of iPP at 177 °C before and after shear at the time indicated, (b) normalized relative intensities of the 998 cm^{-1} band vs time after shear at the temperatures indicated, (c) the relaxation time of the 998 cm^{-1} band at different temperatures after shear, and (d) normalized relative intensities of the 998 cm^{-1} band vs time after shear at 168 °C (shear rate of 13.5 s^{-1}, and shear strain of 3375%).

the COR increases almost linearly with shear rate, whereas an upturn of the COR occurs at low shearing temperatures, which may be related to the positive feedback of the formation of the so-called precursor or nuclei for crystallization. Nevertheless, the effect of temperature on the shear-induced COR is manifested again, as shown in Figure 2. Connected to the temperature effect, it also implies that high shear rate at high temperature may have the same effect as low shear rate at low temperature.

Relaxation of Conformational Order. As shown in Figures 1b and 5a, relaxation of conformational order occurs after shear. The intensity of the vibration band first goes through a fast decrease, followed by a slow one. There is almost no difference with the spectra of the original data before shear after 1800 s of relaxation. Figure 5b shows a series of normalized intensities

of the 998 cm^{-1} band obtained after shear (shear rate of 13.5 s^{-1} and shear strain of 3375%) at different temperatures. The relaxation process was analyzed at temperatures above the normal melting point (165 °C) to avoid interference from crystallization, which leads to a deviation of the relaxation process.

Taking the relaxation process as a helix−coil transition, we employed the model widely used in protein.[43]

$$h(t) = h_{eq} + \Delta h_1 \exp\left(-\frac{t}{\tau_1}\right) \quad (1)$$

where h is the fraction of helix and h_{eq} is the equilibrium fraction helix at the temperature of the isothermal experiment, Δh_1 is the difference between the starting and the equilibrium values of the fraction helix, and τ_1 is the relaxation time. The fitting result τ_1 is plotted versus $1/T$ as an Arrhenius-type curve in Figure 5c. A linear fitting gives an apparent activation energy of 135 kJ/mol for the helix−coil transition, which is about double the value obtained by Zhu and Yan with the Snyder method.[44,45] Evidently at low temperature, the curve deviates from a linear relation, where the relaxation time τ_1 shows a sharp increase. Indeed at temperature higher than around 170 °C, the relaxation kinetics fits well to the first-order exponential decay, whereas at lower temperature the relaxation kinetics does not obey well with it. The slowing down of the relaxation may connect with the so-called precursor. Isolated single helices and helices inside the so-called precursor are expected to have different relaxation kinetics. Thus, the second-order exponential function

$$h(t) = h_{eq} + \Delta h_1 \exp\left(-\frac{t}{\tau_1}\right) + \Delta h_2 \exp\left(-\frac{t}{\tau_2}\right) \quad (2)$$

is tentatively used to fit the relaxation kinetics at low temperatures. Here τ_2 and Δh_2 are the relaxation time and the helix fraction in the so-called precursors. A comparison of the fitting results with the eqs 1 and 2 on the relaxation kinetics at 168 °C is presented in Figure 5d. Obviously, the second-order exponential decay is more suitable at this temperature, which generates τ_1 of 315 s and τ_2 of 16 428 s. This indicates these helices inside the so-called precursors are extremely stable at low temperature though no crystallization occurs. It is certainly unwise to declare that a sharp-cut temperature exists for the occurrence of the helical bundles. Though we fit the relaxation at high temperatures with the first-order exponential decay, some helical bundles may still occur. At temperatures where iPP can easily crystallize, it is difficult to have a complete relaxation to reach the status before shear. Taken 156 °C as an example, 30% of the COR still remains in the melt at the onset of crystallization.

Correlation between Shear-Induced Conformational Ordering and Crystallization. By imposing shear at low temperature where iPP can crystallize, we can correlate the shear-induced crystallization with the COR. Figure 6a shows the evolution of the intensity of the 998 cm^{-1} band before and after shear at 131 °C. In order to emphasize the effect of shear on conformational order, data during crystallization at longer time is not shown. Figure 6b plots the half-time of crystallization versus the COR. The half-time of crystallization decreases with an increasing COR. It is generally accepted that shear-induced crystallization is mainly due to the increase of nuclei. The number of helices inside the precursors plays an important role for the acceleration of the crystallization rate, though we cannot assign how many shear-induced helices locate in the precursors and the average size of it.

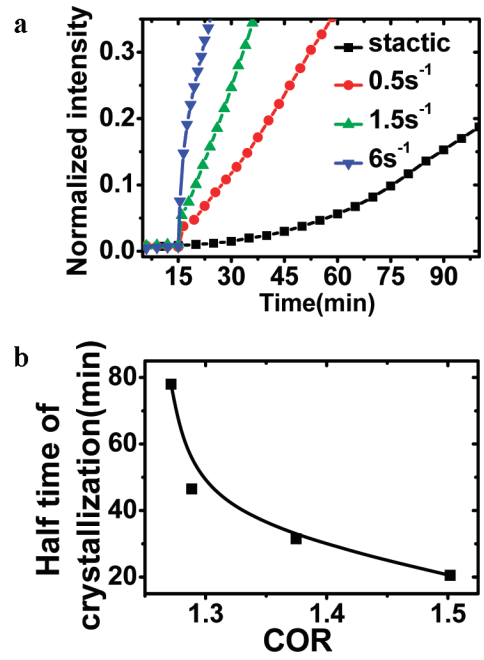

Figure 6. (a) Normalized intensities of the 998 cm^{-1} band vs time and (b) half-time of crystallization vs conformational order ratio (COR) after shear pulses at 131 °C. The shear strain is 4500%, and shear rates are indicated in the figure.

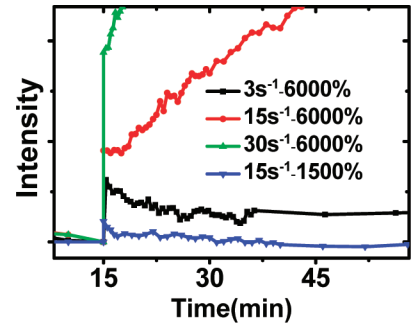

Figure 7. Intensities of the 998 cm^{-1} band vs time before and after shear pulses at 157 °C. The parameters of shear pulses are indicated in the figure.

At smaller supercooling, the competition between relaxation and crystallization is more clearly demonstrated. Figure 7 shows the evolution of the intensity of the 998 cm^{-1} band with different shear pulses at 157 °C. We use intensity rather than normalized intensity because the time is too long to get fully crystallized before thermal degradation.

It is clear to see that shear leads to a sharp increase in intensity of the 998 cm^{-1} bands after shear. Higher shear rate (30 s^{-1}) with the same strain (6000%) or larger shear strain (6000%) with the same shear rate (15 s^{-1}) has a larger influence, which was also evidenced by Figures 3 and 4 before. It is interesting to notice that the sharp increase in intensity of the 998 cm^{-1} band continued after shear at larger COR (shear rate of 30 s^{-1} and shear strain of 6000%) but showed a relaxation at a lower COR, which was induced by a lower shear rate (shear rate of 3 s^{-1} and shear strain of 6000%) or a smaller shear strain (shear rate of 15 s^{-1} and shear strain of 1500%). This phenomenon can be extended to a wide temperature range below the melting point. The results lead to three different crystallization processes connected to different temperatures and shear pulses. (i) The shear-induced crystallization takes place directly after shear-induced conformational ordering without a relaxation and rearrangement process. (ii) Crystallization occurs after some

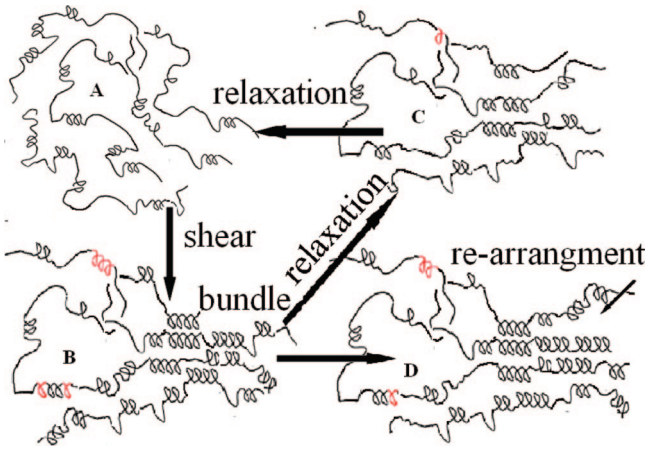

Figure 8. Schematic picture of shear-induced conformational ordering, relaxation, and crystallization.

relaxation of the shear-induced helices, but the COR still remains larger than 1 in the melt before crystallization. This implies that shear-induced conformational ordering still plays an important role at the crystallization. (iii) The occurrence of crystallization is after whole relaxation of the shear-induced helices. Shear-induced conformational order almost relaxed back to reach the status before shear. There is almost no difference comparing to the static condition.

Combining Figures 6a and 7, it also implies that different shear may have the same behavior as the effect of supercooling. At a certain temperature, there exits a critical shear rate or strain connected with COR to "effectively" induce crystallization before being totally relaxed back, which increases with increasing temperature.

Discussion

On the basis of the above results about shear-induced conformational ordering, relaxation, and crystallization, it is possible to construct a simple model to describe this process, which is schematically illustrated in Figure 8. Starting with short helices and coils (Figure 8A),[40] it is necessary to notice that the "coil" here is used to describe short-range conformational disorder, which was different from the Gaussian random coil. Shear increases the concentration of long helices (the red helices in Figure 8B) through nucleation (the rate-limiting formation of the first helical turn) or propagation (fast addition of helical residues to its ends).[8,46] Without such primary nucleation the short helices would be consumed by the formation of longer ones, leading to a decrease of their concentration. As all conformational bands show an increase of intensity after shear, we can safely conclude that nucleation does happen. In addition to nucleation and growth as well as subsequent propagation, a third possibility for the formation of long helices is by merging two shorter ones (incorporation), which can diffuse along the molecular chain without energy barrier.[47] There are two kinds of helices: (i) isolated single helices far away from each other without interactions; (ii) clusters of helices or helical bundles with interactions among each other. After the cessation of shear, both of them face two destinies: to relax back to random coil into the amorphous melt (Figure 8C) or to survive and grow by rearrangement and induce crystallization (Figure 8D), which depends on different temperatures and shear. We discuss the shear-induced conformational ordering, relaxation, and crystallization in the following.

Shear-Induced Conformational Ordering. Shear-induced conformational ordering strongly depends on temperature, shear rate, and strain. The effect of shear becomes smaller with rising temperature (see Figure 2). There is hardly any detectable change above 205 °C. As the diffusion coefficient of the molecular chain is proportion $\exp(-\Delta E_a/RT)$, where ΔE_a and R are the activation energy for diffusion and the gas constant, respectively, chains relax back faster at higher temperatures. It is more difficult for them to build orientation and stretch with the same shear field at high temperatures. Nevertheless, the sharp increase of the COR at low temperatures could not be explained by temperature dependence of chain relaxation alone. A positive feedback through the formation of helical aggregates may occur at low temperatures, which not only stabilizes the helices, but also helps chains to build orientation and stretch, and further generates more ordered conformations. The sharp dropdown at high temperatures is not clear to us yet. It may be due to experimental uncertainty because the low viscosity at high temperatures prevents us from better controlling the shearing experiments.

Following the theory on the stretch-induced coil−helix transition of a single chain and network,[9−13] it is possible to describe the shear-induced coil−helix transition in iPP, as a polymer melt is essentially a network with entangled chains. The free energy F_{ch} of a single chain with helical and coil segments can be expressed as the following function:

$$F_{ch} = \chi N\Delta f + 2\Delta f_t + \frac{3(r-\gamma aN\chi)^2}{2(1-\chi)Na^2} \qquad (3)$$

where Δf and Δf_t are the free energy of the helix and the interface free energy between helix and coil segments, respectively. N and a are the total number and the length of the monomer, respectively. r is the end−end distance of the chain. χ is the fraction of helix in one chain, which has a value from 0 to 1. γ is the geometric factor accounting for the helix length, per monomer. The last term of the equation is the entropy of the coil segments. Shear is expected to increase r and reduce the entropy of the coil segments, provided the shear rate is fast enough to overcome the relaxation of chain. A threshold of extension of the chain may be required to induce the coil−helix transition.[12] This is confirmed by the result in Figure 3 where a detectable induced conformational ordering occurs with a strain larger than a minimum value. The overall profile of the plot of the COR versus the strain in Figure 3 matches well with the prediction of theory on the coil−helix transition of the network induced by stretch (see Figure 2 of ref 12).

Unlike in the permanently cross-linked network, entangled chains in the polymer melt can enjoy their freedom to relax back to their equilibrium coil state. Thus, the effect of shear rate on the coil−helix transition comes in. The coil−helix transition in a permanent network can be treated as a quasi-thermodynamic process provided the stretching rate is slow enough, whereas it is a nonthermodynamic process in the entangled polymer melt. With a larger shear rate, the end-to-end distance r is expected to be larger than that with a smaller shear rate even though the same strain is imposed (see Figure 4). Taking into account the competition between relaxation and extension induced by shear, an "effective strain" of the individual molecular chain is the actual parameter to correlate with the COR.

We would like to mention two important aspects which may need further development. (i) Though the theory on the stretch-induced conformational ordering in the network can be borrowed to explain the coil−helix transition in polymer melt qualitatively, it does not take into account the coupling among helices, which does occur in polymers melt around the crystallization temper-

atures (see the next section). The free energy expression in eq 3 is for a single chain. It does not incorporate the interhelix interaction, which generally lowers down the free energy more significantly than intrachain ordering and is an essential step to construct precursors or nuclei for crystallization. (ii) One important progress in rheology of polymer prevents us from quantitatively analyzing the correlation between the time scale between relaxation time (both Rouse time τ_R and reptation time τ_r) with shear rate. The heterogeneity of shear flow in terms of space, frequency, and time may lead any simple comparison of the experimental time scale and molecular dynamic to be uncertain.[48]

Relaxation of Conformational Order. The conformational order induced by shear is a nonthermodynamic process. After the cessation of shear, helices face two destinies: rearranging and growing or relaxing back, which is determined by temperature and shear. The effect of temperature on the relaxation kinetics suggests that there are two different helical states, namely, isolated single helices and helical bundles induced by shear (see Figure 8B). As the involvement of interhelical interaction, the relaxation of helices inside the bundles takes a cooperative approach, which is much slower than that of the isolated single helices. At high temperatures, a single fast relaxation kinetics indicates that the isolated single helices are the main product. This result is consistent with the COR. At high temperatures, there are a few induced long helices and consequently a low probability to form the helical bundles. The relaxation time of single helix at high temperature is near 200 s, which is still rather long compared to the average reptation time τ_r. This is natural as the "melting" of helices involves not only an entropy effect but also enthalpy. The latter may delay the relaxation process.

It is a different scene at low temperatures (above the melting temperature). Higher concentration of the induced helices leads to a higher possibility to form large and compact helical bundles. Once formed, the bundles can lower their free energy and be stabilized (see Figure 8D). At low temperatures (see Figure 5d), the slow relaxation process indicates that the helical bundles are the dominant state, provided the shear pulse is sufficient. Within our experimental time (3 h), helices even do not relax completely back to their equilibrium state.[49] Though we discuss that the helices with intersegment interactions are more stable than the isolated helices in general, helical bundles with different sizes and internal arrangements are expected to have different stabilities. This difference leads to the two destinies below the melting temperature of iPP (see Figure 8, parts C and D). Helical bundles with smaller size and more misarrangements are more likely to relax back or crystallize after necessary arrangement (Figure 8C), whereas the larger helical bundles with closer packing have a higher possibility to have a local volume with the "right" arrangement, which can induce crystallization directly at low temperature (Figure 7).

The scale of the relaxation times at low and high temperatures suggests any stable or metastable structures require the coupling between the intrachain conformational and interchain orientational and positional order in iPP. At high temperatures, helices relax back completely after the cessation of shear, which is a thermodynamic reversible process (though it is induced through a nonthermodynamic process). The isolated single long helices are not stable or metastable at high temperatures.

Correlation between Shear-Induced Conformational Order and Crystallization. How does the shear-induced conformational order relate to crystallization? Our result implies that the shear-induced conformational order plays an important role in crystallization. However, if concentration and length of the helical sequences were the only critical parameters for crystallization, one would always expect iPP to crystallize directly after shear when these parameters are larger than that after some relaxation. The occurrence of crystallization after relaxation of the shear-induced helices suggests that a rearrangement of the helices is necessary.[50] The packing of helices rather than helices themselves may be the essential difference between the shear-induced precursors and nuclei or shish. Shear can generate four types of helical hands (left- and right-handed helices as well as "up" and "down" positions concerning the CH_3 group) in a short time. However, it will take much longer time for these four types of helices to sort out a specific spatial arrangement as that in a crystal which requires precisely the handedness alternation. As the result of shear, a collection of chain stems with different hands but uniform direction is formed in the helical bundles. In other words, the shear-induced precursors consist primarily of the so-called "mesomorphic" or "liquid crystal" phase structure. This structure undergoes a perfection process through melting/reforming and rearranging of helices, which generates nuclei or shish for the future stem-by-stem deposition process (crystallization).

How many stems are required to form a stable precursor or shish?[51] Do they have a uniform size? Our results cannot answer the first question, but the plot of the COR versus half-time of crystallization in Figure 6b may gives some indications to the second one. Assuming that the major part of the induced helices participates into the precursor and later into the shish at this low temperatures, the number of shish with uniform size will be proportional to the COR. This reasoning leads to a power law between the growth rate and the COR, which is determined by the growth fashion in two or three dimensions. This power law is not found from Figure 6b, though the crystallization time does monotonically decrease with the increase of the COR. A rough estimation on the correlation between the shear-induced helices and corresponding crystallization rates implies that a larger shear rate or strain induces not only a higher density but also a larger size (more stems) of helical bundles.

Conclusion

In situ FTIR measurements reveal that conformational order can be induced in the iPP melt by shear. The effect is more pronounced at temperatures below the melting point of iPP than above. Following the shear-induced conformational ordering, relaxation as well as crystallization occurs, which strongly depend on temperature and shear pulse. The lifetime of the nucleation precursors is a very sensitive function of relaxation temperature. Two different relaxation kinetics exist when it comes to different temperatures. Though there is no distinct boundary, the first-order exponential decay seems to fit well on the relaxation at the high temperatures, whereas it is obviously the second-order exponential decay at temperatures around the normal melting point of iPP. The shorter relaxation time comes from rapid unzipping of the isolated single helices, whereas the longer relaxation time results from the helices contained in bundles. The precursors of nuclei consist primarily of the so-called "mesomorphic" or "liquid crystal" phase structure. It takes time for the helices to arranging for future stem-by-stem deposition process. The different helix concentrations and their distribution are the origin of the three different crystallization behaviors after shear. The competition of conformational relaxation and crystallization suggests that conformational ordering alone is not sufficient to induce crystallization.

Acknowledgment. We thank Professor Wim de Jue (AMOLF), Professor Yukihiro Ozaki (Kwansei Gakuin University), Professor Xinyuan Zhu (Shanghai Jiaotong University), and Professor Shaw Ling Hsu (UMass) for fruitful discussion. This work is supported by the National Natural Science Foundation of China (50503015 and international collaboration fund) as well as the "NCET" program of the Minister of Education. The research is also in part supported by the Opening Project of the State Key Laboratory of Polymer Materials Engineering (Sichuan University).

References and Notes

(1) Nakatani, A. I.; Dadmun, M. D. *Flow-Induced Structure in Polymer*; American Chemical Society: Washington, DC, 1995.
(2) Li, L. B.; De Jeu, W. H. *Adv. Polym. Sci.* **2005**, *181*, 75.
(3) Somani, R. H.; Yang, L.; Zhu, L.; Hsiao, B. S. *Polymer* **2005**, *46*, 8587.
(4) Auriemma, F.; De Rosa, C.; Corradini, P. *Adv. Polym. Sci.* **2005**, *181*, 1.
(5) Bermejo, F. J.; Criado, A.; Fayos, R.; Fernandez, P. R.; Fischer, H. E.; Suard, E.; Guelylah, A.; Zuniga, J. *Phys. Rev. B* **1997**, *56*, 11536.
(6) Wunderlich, B.; Grebowicz, J. *Adv. Polym. Sci.* **1984**, *60*, 1.
(7) Saenger, W. *Principles of Nucleic Acid Structure*; Springer-Verlag: New York, 1984.
(8) An, H. N.; Zhao, B. J.; Ma, Z.; Shao, C. G.; Wang, X.; Fang, Y. P.; Li, L. B.; Li, Z. M. *Macromolecules* **2007**, *40*, 4740.
(9) Buhot, A.; Halperin, A. *Phys. Rev. Lett.* **2000**, *84*, 2160.
(10) Buhot, A.; Halperin, A. *Macromolecules* **2002**, *35*, 3238.
(11) Tamashiro, M. N.; Pincus, P. *Phys. Rev. E* **2001**, *63*, 021909.
(12) Courty, S.; Gornall, J. L.; Terentjev, E. M. *Proc. Natl. Acad. Sci. U.S.A.* **2005**, *102*, 13457.
(13) Courty, S.; Gornall, J. L.; Terentjev, E. M. *Biophys. J.* **2006**, *90*, 1019.
(14) Terrill, N. J.; Fairclough, P. A.; Ryan, A. J. *Polymer* **1998**, *39*, 2381.
(15) Isayev, A. I.; Chan, T. W.; Shimojo, K.; Gmerek, M. *J. Appl. Polym. Sci.* **1995**, *55*, 807.
(16) Chai, C. K.; Dixon, N. M.; Gerrard, D. L.; Reed, W. *Polymer* **1995**, *36*, 661.
(17) Pogodina, N. V.; Siddiquee, S. K.; Van Egmond, J. W.; Winter, H. H. *Macromolecules* **1999**, *32*, 1167.
(18) Pogodina, N. V.; Winter, H. H. *Macromolecules* **1998**, *31*, 8164.
(19) Pogodina, N. V.; Lavrenko, V. P.; Srinivas, S.; Winter, H. H. *Polymer* **2001**, *42*, 9031.
(20) Kumaraswamy, G.; Varma, R. K.; Issaian, A. M.; Kornfield, J. A.; Yeh, F.; Hsiao, B. S. *Polymer* **2000**, *41*, 8931.
(21) Kumaraswamy, G.; Issaian, A. M.; Kornfield, J. A. *Macromolecules* **1999**, *32*, 7537.
(22) Somani, R. H.; Yang, L.; Hsiao, B. S. *Physica A* **2002**, *304*, 145.
(23) Somani, R. H.; Hsiao, B. S.; Nogales, A.; Srinivas, S.; Tsou, A. H.; Sics, I.; Baltá-Calleja, F. J.; Ezquerra, T. A. *Macromolecules* **2000**, *33*, 9385.
(24) Somani, R. H.; Hsiao, B. S.; Nogales, A.; Fruitwala, H.; Srinivas, S.; Tsou, A. H. *Macromolecules* **2001**, *34*, 5902.
(25) Somani, R. H.; Yang, L.; Hsiao, B. S.; Fruitwala, H. *J. Macromol. Sci., Phys.* **2003**, *B42*, 515.
(26) Somani, R. H.; Sics, I.; Hsiao, B. S. *J. Polym. Sci., Part B: Polym.Phys.* **2006**, *44*, 3553.
(27) Azzurri, F.; Alfonso, G. C. *Macromolecules* **2005**, *38*, 1723.
(28) Zuo, F.; Keum, J. K.; Yang, L.; Somani, R. H.; Hsiao, B. S. *Macromolecules* **2006**, *39*, 2209.
(29) De Gennes, P. G.; Pincus, P. *Polym. Prepr. (Am. Chem. Soc., Div. Polym. Chem.)* **1977**, *18*, 161.
(30) Flory, P. J.; Matheson, R. R., Jr *J. Phys. Chem.* **1984**, *88*, 6606.
(31) Matsuba, G.; Kaji, K.; Nishida, K.; Kanaya, T.; Imai, M. *Macromolecules* **1999**, *32*, 8932.
(32) Tashiro, K.; Sasaki, S.; Kobayashi, M. *Macromolecules* **1996**, *29*, 7460.
(33) Tashiro, K.; Sasaki, S.; Gose, N.; Kobayashi, M. *Polym. J.* **1998**, *30*, 85.
(34) Sasaki, S.; Tashiro, K.; Kobayashi, M.; Izumi, Y.; Kobajashi, M. *Polymer* **1999**, *40*, 7125.
(35) Suter, U. W.; Flory, P. J. *Macromolecules* **1975**, *8*, 765.
(36) Tonelli, A. E. *Macromolecules* **1972**, *5*, 563.
(37) Zerbi, G.; Ciampelli, F.; Zamboni, V. *J. Polym. Sci.* **1963**, *C7*, 141.
(38) Kissin, Y. V.; Tsvetkova, V. I.; Chirkov, N. M. *Eur. Polym. J.* **1972**, *8*, 529.
(39) Miyamoto, T.; Inagaki, H. *J. Polym. Sci.* **1969**, *7*, 963.
(40) Zhu, X. Y.; Yan, D. Y.; Fang, Y. P. *J. Phys. Chem. B* **2001**, *105*, 12461.
(41) Budevska, B. O.; Manning, C. J.; Griffiths, P. R.; Roginski, R. T. *Appl. Spectrosc.* **1993**, *47*, 1843.
(42) Painter, P. C.; Colemman, M. M.; Koening, J. L. *The Theory of Vibrational Spectroscopy and Its Application to Polymeric Materials*; John Wiley & Sons: New York, 1982; p 382.
(43) Persikov, A. V.; Xu, Y.; Brodsky, B. *Protein Sci.* **2004**, *13*, 893.
(44) Zhu, X. Y.; Yan, D. Y. *Macromol. Chem. Phys.* **2001**, *202*, 1109.
(45) Hagemann, H.; Strauss, H. L.; Snyder, R. G. *Macromolecules* **1987**, *20*, 2810.
(46) Poland, D.; Scheraga, H. A. *Theory of Helix−Coil Transitions in Biopolymers*; Academic Press: New York, 1970.
(47) Hummer, G.; Garcia, A. E.; Garde, S. *Phys. Rev. Lett.* **2000**, *85*, 2637.
(48) Wang, S. Q.; Ravindranath, S.; Wang, Y. Y.; Boukany, P. Y. *J. Chem. Phys.* **2007**, *127*, 064903.
(49) Na, B.; Wang, Y.; Zhang, Q.; Fu, Q. *Polymer* **2004**, *45*, 6245.
(50) Yamazaki, S.; Watanabe, K.; Okada, K.; Yamada, K.; Tagashira, K.; Toda, A.; Hikosaka, M. *Polymer* **2005**, *46*, 1685.
(51) Chen, E.; Weng, X.; Zhang, A.; Mann, I.; Harris, F. W.; Cheng, S. Z. D.; Stein, R. S.; Hsiao, B. S.; Yeh, F. J. *Macromol. Rapid Commun.* **2001**, *22*, 611.

JP802511B